Electronic Supplementary Material (ESI) for Nanoscale.

Supporting Information Available

Silica Nanonetwork Confined in Nitrogen-Doped Ordered Mesoporous Carbon Framework for High-Performance Lithium-Ion Battery Anodes

Yeru Liang[a†], Lifeng Cai[b†], Luyi Chen,[a] Xidong Lin[a], Ruowen Fu[a*], Mingqiu Zhang[a], Dingcai Wu[a*]

[a] *Materials Science Institute, PCFM Lab and GDHPPC Lab, School of Chemistry and Chemical Engineering, Sun Yat-sen University, Guangzhou, 510275, P. R. China*

[b] *School of Environmental and Biological Engineering, Putian University, Putian 351100, P. R. China*

Experimental Section

Sample Preparation: The N-OMC/SiO_2 sample was prepared by a well-known multi-constituent co-assembly approach developed by Zhao's group.[1] In a typical synthesis, 0.61 g of phenol was melted in a flask and mixed with 0.13 mL of 5 mol/L NaOH aqueous solution under stirring. Then, 1.05 g of 37 wt.% formaldehyde solution was added. Subsequently, the clear mixture was reacted under stirring for 1 h at 70 ^{o}C and then was cooled to room temperature. The pH was adjusted to ~7.0 by 5 mol/L HCl aqueous solution. The final product was dissolved in ethanol to obtain 10 ml of resol resin solution. Meanwhile, 1.8 g of triblock copolymer (Pluronic F127,

---

* Corresponding authors, E-mail: wudc@mail.sysu.edu.cn (D. Wu); cesfrw@mail.sysu.edu.cn (R. Fu). † Y. R. Liang and L. F. Cai contributed equally to this work.

EO_{106}-PO_{70}-EO_{106}) was dissolved in 10 ml of ethanol with 1 ml of 0.2 mol/L HCl aqueous solution under stirring, followed by mixed with 0.2 g of urea. Subsequently, 2 ml of tetraethyl orthosilicate and the above resol solution were added into the mixture under string in sequence. The obtained homogeneous mixture was transferred to a dish and evaporated for about 8 h at room temperature, followed by heating for 24 h at 100 ^{o}C. The as-prepared product was scraped from the dishes and then carbonized in a tubular furnace for 3 h at 900 ^{o}C under N_2 flow, leading to formation of nitrogen-doped ordered mesoporous carbon/silica nanocomposite. The heating rate was 1 ^{o}C/min below 600 ^{o}C and then was increased to 5 ^{o}C/min above 600 ^{o}C. For comparison, the ordered mesoporous carbon/silica (OMC/SiO_2) without nitrogen-doping was also prepared. Its preparation procedure was exactly the same as that of the N-OMC/SiO_2, except that the addition of urea were bypassed.

Structural Characterization: The thermogravimetric analysis (TGA) was performed by using a TGA Q50 thermogravimetric analyzer (TA Instruments). XRD patterns were recorded on a D-MAX 2200 VPC diffractometer using Cu Kα radiation (40 kV, 26 mA). The elemental analysis was performed on an Elementar Analysensysteme GmbH Vario EL analyzer. XPS measurements were carried out with an ESCALAB250 instrument. The morphologies of the samples were observed by a Hitachi S4800 scanning electron microscope (SEM) and a FEI Tecnai G2 Spirit transmission electron microscope (TEM), and the energy-dispersive spectroscopy and EELS mapping images were detected by a FEI Tecnai G2 F30TEM. The Fourier-transform infrared (FTIR) measurements of the samples were performed with

IR spectroscopy (Bruker TENSOR 27), using KBr disk method. A Micromeritics ASAP 2020 surface area and porosity analyzer was used to investigate the pore structure. The BET surface area (S_{BET}) was analyzed by Brunauer-Emmett-Teller (BET) theory. The external surface area (S_{ext}) was determined by t-plot theory, and then the micropore surface area (S_{mic}) was obtained by subtracting the S_{ext} from the S_{BET}. The total pore volume (V_t) was calculated from the amount adsorbed at a relative pressure P/P_0 of 0.997. The micropore volume (V_{mic}) and the mesopore volume (V_{mes}) were determined by t-plot theory and BJH method, respectively. The pore size distribution was analyzed by original density functional theory (DFT) assuming slit pore with non-negative regularization and medium smoothing.

Electrochemical Characterization: The electrochemical performance of the samples was measured in 2032 coin cells. Li metal was used as counter/reference electrode. The working electrode was made of activate materials (80 wt%), super P (10 wt%) and polyvinylidene fluoride (PVDF) (10 wt%) slurry coated onto a copper foil substrate. The electrodes were cut into circular disks with a diameter of 12 mm and an active material loading density of about 0.3 mg/cm^2. The electrolyte was 1 mol/L $LiPF_6$ in a mixture of ethylene carbonate (EC), dimethyl carbonate (DMC) and Diethyl carbonate (DEC) (1:1:1 by volume). A microporous membrane (Celgard 2300) was used as the separator. The coin cells were assembled in an argon filled glove box (Mbraun). The galvanostatic charge/discharge tests were conducted in the potential range from 0.01 to 3.0 V at different current densities.

Table S1 Pore structure parameters of N-OMC/SiO_2 nanocomposite.

S_{BET} (m^2/g)	S_{ext} (m^2/g)	S_{mic} (m^2/g)	V_t (cm^3/g)	V_{mic} (cm^3/g)	V_{mes} (cm^3/g)
524	386	138	0.53	0.06	0.54

Table S2 Elemental composition information of N-OMC/SiO_2 and OMC/SiO_2 nanocomposites.

Sample	XPS				Elemental analysis		
	C (at%)	N (at%)	Si (at%)	O (at%)	C (wt%)	N (wt%)	H (wt%)
N-OMC/SiO_2	63.6	2.3	7.9	26.2	42.6	6.3 [a]/2.9 [b]	1.2
OMC/SiO_2	—	—	—	—	45.3	0	2.5

[a] Calculated based on the weight of carbon framework; [b] Calculated based on the total weight of N-OMC/SiO_2 nanocomposite.

Table S3 Approximate distribution of N-OMC/SiO_2 nanocomposite.

Sample	N-Q (at%)	N-5 (at%)	N-6 (at%)	N-X (at%)
N-OMC/SiO_2	40	17	15	28

Table S4 Comparison of the cycling performance of some SiO_2-based materials as lithium-ion battery anodes in the literatures.

Item	Stable Capacity (mAh/g)	Cycle Number	Charge/Discharge Rate	Voltage Range (V)	Ref.
SiO_2 thin film	416	100	28 μA/cm^2	0.01~3	[2]
SiO_2/Cu/PAN-C	450	185	110 mA/g	0~3	[3]
Carbon coated TiO_2/SiO_2 composites	272	200	30 mA/g	0~3	[4]
Carbon-coated SiO_2 nanoparticles	500	50	50 mA/g	0~3	[5]
Nano-SiO_2/hard carbon composites	630	14	0.1 mA/cm^2	0~3	[6]
24 h milled SiO_2	*ca.* 700	250	100 mA/g	0~2	[7]
36 h milled SiO_2	*ca.* 600	25			
Pristine SiO_2	*ca.* 100	25			
SiO_2/C composites without ball milling	100	50	100 mA/g	0.01~2.5	[8]
SiO_2/C composites with ball milling	600	100			
Hollow porous SiO_2 nanocubes	919	30	100 mA/g	0~3	[9]
	377	25	500 mA/g		
Hollow triple-shelled SiO_2/TiO_2/polypyrrole nanospheres	424	50	44 mA/g	0.01~3	[10]
Hollow silica nanospheres	359	100	1 C	0~2.5	[11]
Dense silica powder	*ca.*100	25			
N-OMC/SiO_2 nanocomposite	800	20	200 mA/g	0.01~3	This work
	658	100			

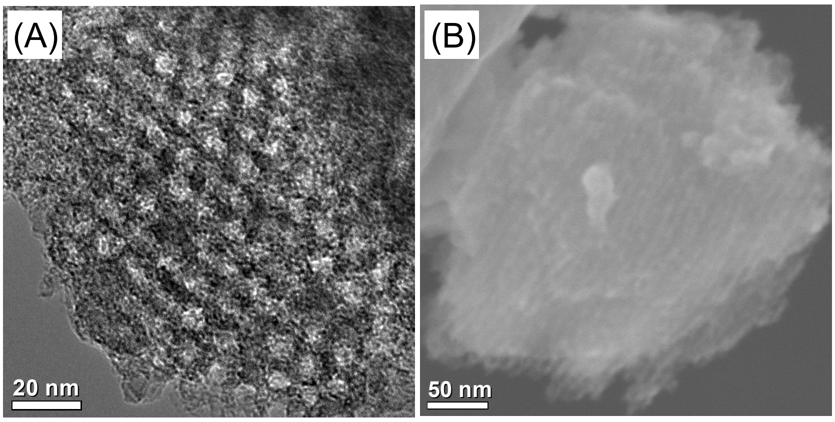

Fig. S1 (A) TEM image and (B) SEM image of N-OMC/SiO_2 nanocomposite.

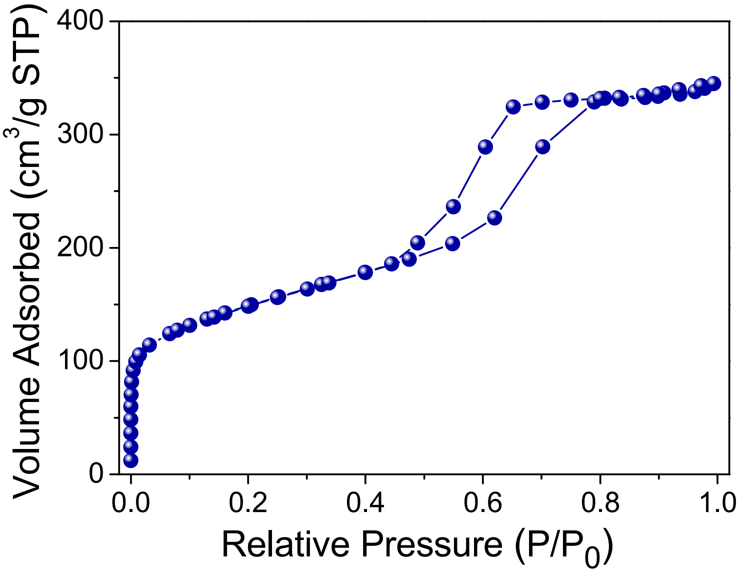

Fig. S2 N_2 adsorption-desorption isotherm of N-OMC/SiO_2 nanocomposite.

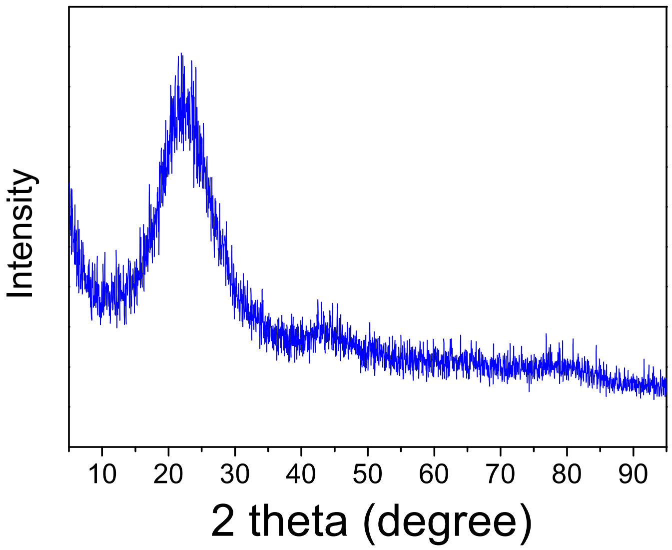

Fig. S3 Wide-angle XRD pattern of N-OMC/SiO_2 nanocomposite.

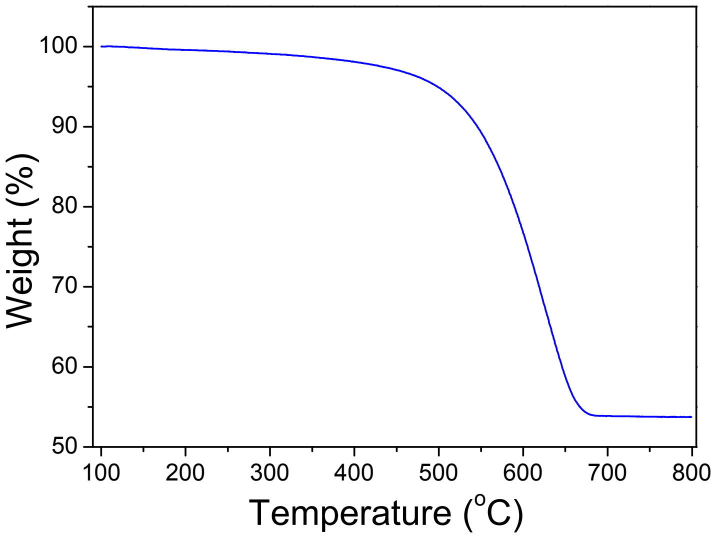

Fig. S4 TGA curve of N-OMC/SiO_2 nanocomposite conducted in air.

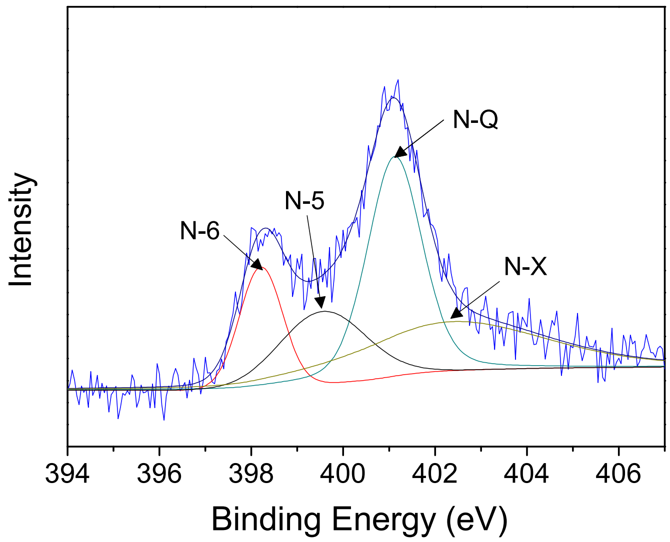

Fig. S5 XPS spectrum for the N1s region of N-OMC/SiO_2 nanocomposite.

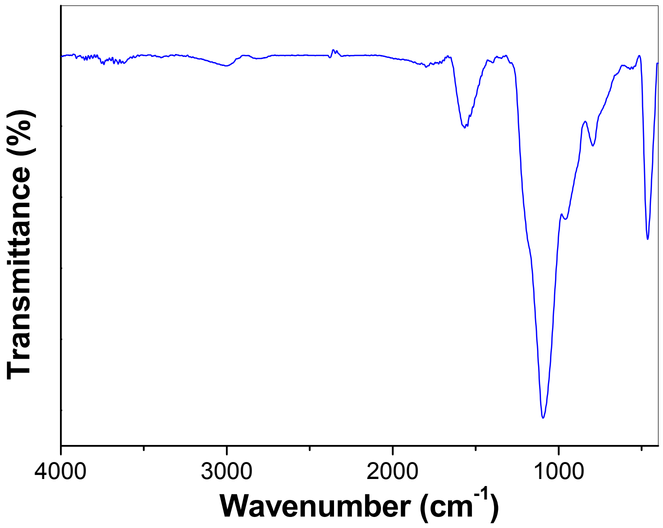

Fig. S6 FTIR spectrum of N-OMC/SiO_2 nanocomposite.

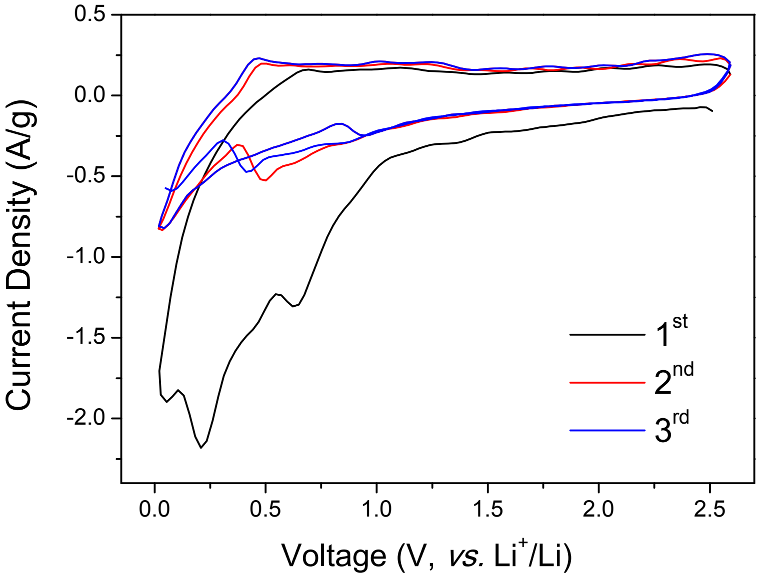

Fig. S7 Cyclic voltammogram curves of N-OMC/SiO_2 nanocomposite electrode at 0.1 mV/s.

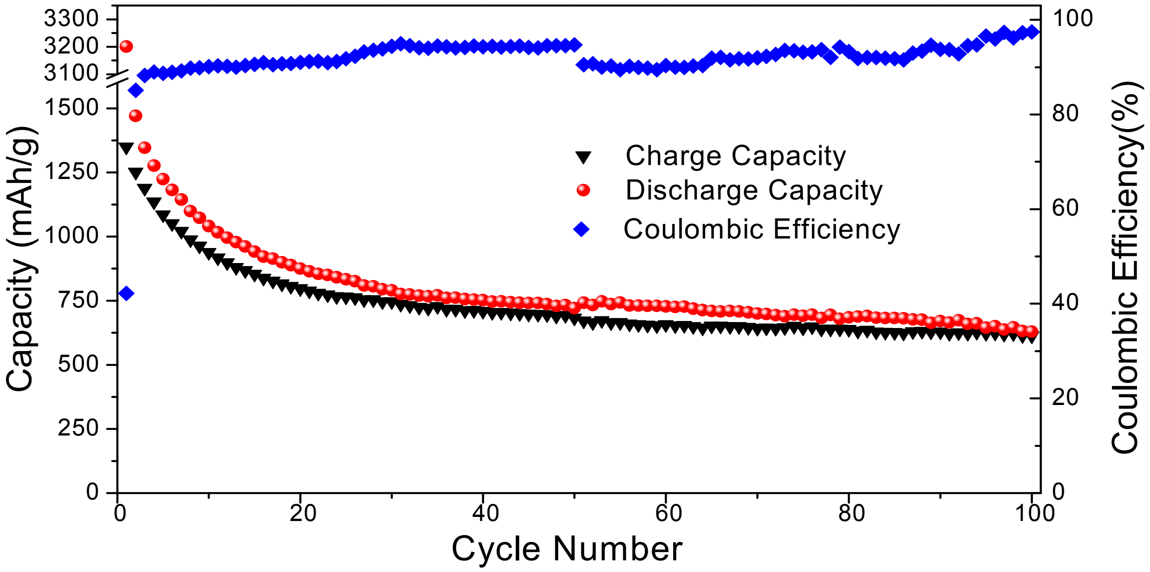

Fig. S8 Cyclability and Coulombic efficiency of N-OMC/SiO_2 nanocomposite electrode at 100 mA/g.

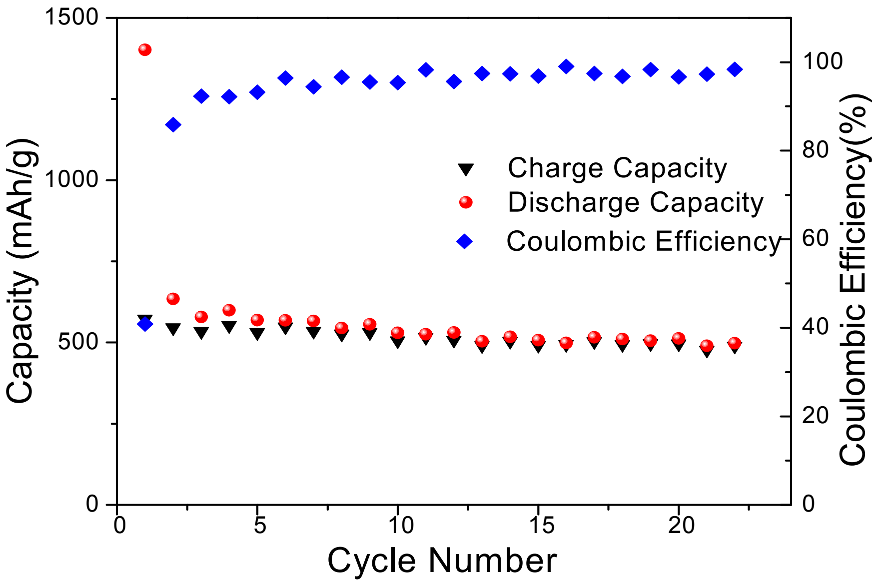

Fig. S9 Cyclability and Coulombic efficiency of OMC/SiO_2 nanocomposite electrode at 100 mA/g.

References

1. Liu, R.; Shi, Y.; Wan, Y.; Meng, Y.; Zhang, F.; Gu, D.; Chen, Z. Tu, B.; Zhao, D. Triconstituent co-assembly to ordered mesostructured polymer-silica and carbon-silica nanocomposites and large-pore mesoporous carbons with jigh surface areas. *J. Am. Chem. Soc.* **2006**, *128*, 11652-11662.
2. Sun, Q.; Zhang, B.; Fu, Z.-W. Lithium electrochemistry of SiO_2 thin film electrode for lithium-ion batteries. *Appl. Surf. Sci.* **2008**, *254*, 3774-3779.
3. Li, M.; Li, J.; Li, K.; Zhao, Y.; Zhang, Y.; Gosselink, D.; Chen, P. SiO_2/Cu/polyacrylonitrile-C composite as anode material in lithium ion batteries. *J. Power Sources* **2013**, *240*, 659-666.
4. Zhang, J.-J.; Wei, Z.; Huang, T.; Liu, Z.-L.; Yu, A.-S. Carbon coated TiO_2-SiO_2 nanocomposites with high grain boundary density as anode materials for

lithium-ion batteries. *J. Mater. Chem. A* **2013**, *1*, 7360-7369.

5. Yao, Y.; Zhang, J.; Xue, L.; Huang, T.; Yu, A. Carbon-coated SiO_2 nanoparticles as anode material for lithium ion batteries. *J. Power Sources* **2011**, *196*, 10240-10243.
6. Guo, B.; Shu, J.; Wang, Z.; Yang, H.; Shi, L.; Liu, Y.; Chen, L. Electrochemical reduction of nano-SiO_2 in hard carbon as anode material for lithium ion batteries. *Electrochem. Commun.* **2008**, *10*, 1876-1878.
7. Chang, W.-S.; Park, C.-M.; Kim, J.-H.; Kim, Y.-U.; Jeong, G.; Sohn, H.-J. Quartz (SiO_2): a new energy storage anode material for Li-ion batteries. *Energ. Environ. Sci.* **2012**, *5*, 6895-6899.
8. Lv, P.; Zhao, H.; Wang, J.; Liu, X.; Zhang, T.; Xia, Q. Facile preparation and electrochemical properties of amorphous SiO_2/C composite as anode material for lithium ion batteries. *J. Power Sources* **2013**, *237*, 291-294.
9. Yan, N.; Wang, F.; Zhong, H.; Li, Y.; Wang, Y.; Hu, L.; Chen, Q. Hollow porous SiO_2 nanocubes towards high-performance anodes for lithium-ion batteries. *Sci Rep* **2013**, *3*, 1568.
10. Kim, J. M.; Huh, Y. S.; Kim, H. J.; Song, K.; Kim, S. H.; Park, H. S. Hollow triple-shelled SiO_2/TiO_2/polypyrrole nanospheres for enhanced lithium storage capability. *Chem. Eng. J.* **2014**, *237*, 380-386.
11. Sasidharan, M.; Liu, D.; Gunawardhana, N.; Yoshio, M.; Nakashima, K. Synthesis, characterization and application for lithium-ion rechargeable batteries of hollow silica nanospheres. *J. Mater. Chem.* **2011**, *21*, 13881-13888.